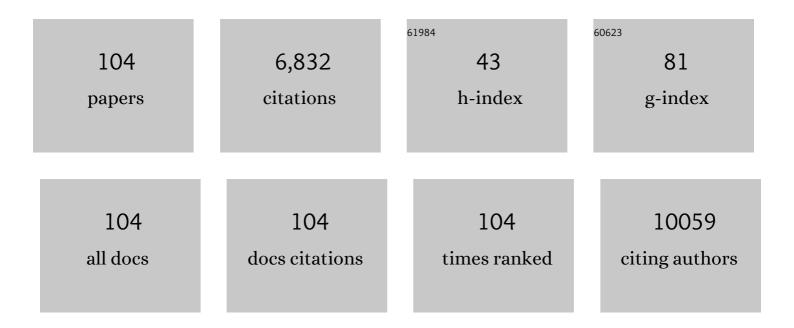
## List of Publications by Year in descending order

Source: https://exaly.com/author-pdf/2091243/publications.pdf Version: 2024-02-01



KE CHEN

#	Article	IF	CITATIONS
1	Mitigating Interfacial Mismatch between Lithium Metal and Garnet-Type Solid Electrolyte by Depositing Metal Nitride Lithiophilic Interlayer. ACS Applied Energy Materials, 2022, 5, 648-657.	5.1	16
2	Enhanced near-field coupling and tunable topological transitions in hyperbolic van der Waals metasurfaces for optical nanomanipulation. Nanoscale, 2022, 14, 7075-7082.	5.6	4
3	Controllable Growth of Graphene Photonic Crystal Fibers with Tunable Optical Nonlinearity. ACS Photonics, 2022, 9, 961-968.	6.6	7
4	Suppressing interface charge recombination for efficient integrated perovskite/organic bulk-heterojunction solar cells. Journal of Power Sources, 2022, 541, 231665.	7.8	6
5	Graphene-integrated waveguides: Properties, preparation, and applications. Nano Research, 2022, 15, 9704-9726.	10.4	7
6	Enhanced Hemocompatibility of a Direct Chemical Vapor Deposition-Derived Graphene Film. ACS Applied Materials & Interfaces, 2021, 13, 4835-4843.	8.0	8
7	Mitigating Open-Circuit Voltage Loss in Pb–Sn Low-Bandgap Perovskite Solar Cells via Additive Engineering. ACS Applied Energy Materials, 2021, 4, 1731-1742.	5.1	43
8	Grain Boundary Defect Passivation in Quadruple Cation Wideâ€Bandgap Perovskite Solar Cells. Solar Rrl, 2021, 5, 2000740.	5.8	19
9	Achieving High Pseudocapacitance Anode by An <i>In Situ</i> Nanocrystallization Strategy for Ultrastable Sodium-Ion Batteries. ACS Applied Materials & Interfaces, 2021, 13, 22577-22585.	8.0	10
10	Solving Lithium Dendrite Problems through Structure Design of Advanced Metal Anodes for Lithium Metal Batteries. ECS Meeting Abstracts, 2021, MA2021-01, 2085-2085.	0.0	0
11	Plasma Oxidized Ti <sub>3</sub> C <sub>2</sub> T <sub><i>x</i></sub> MXene as Electron Transport Layer for Efficient Perovskite Solar Cells. ACS Applied Materials & Interfaces, 2021, 13, 32495-32502.	8.0	41
12	High-mass-loading Sn-based anode boosted by pseudocapacitance for long-life sodium-ion batteries. Chemical Engineering Journal, 2021, 414, 128638.	12.7	29
13	Facile Chemical Fabrication of a Three-Dimensional Copper Current Collector for Stable Lithium Metal Anodes. Journal of the Electrochemical Society, 2021, 168, 070502.	2.9	5
14	Ultraflat Langmuir–Blodgett assembled graphene oxide saturable-absorber films for pulsed near-infrared laser generation. Nanotechnology, 2021, 32, 385709.	2.6	8
15	Advanced strategies for the development of porous carbon as a Li host/current collector for lithium metal batteries. Energy Storage Materials, 2021, 41, 448-465.	18.0	60
16	MOF-derived hierarchical carbon network as an extremely-high-performance supercapacitor electrode. Electrochimica Acta, 2021, 394, 139058.	5.2	67
17	High efficiency photocatalytic reaction dominated by the direct transfer of hot electrons. Physica E: Low-Dimensional Systems and Nanostructures, 2020, 115, 113699.	2.7	0
18	Tailored PEDOT:PSS hole transport layer for higher performance in perovskite solar cells: Enhancement of electrical and optical properties with improved morphology. Journal of Energy Chemistry, 2020, 44, 41-50.	12.9	105

#	Article	IF	CITATIONS
19	One-pot synthesis of 3D Au nanoparticle clusters with tunable size and their application. Nanotechnology, 2020, 31, 085601.	2.6	3
20	A copper-clad lithiophilic current collector for dendrite-free lithium metal anodes. Journal of Materials Chemistry A, 2020, 8, 1911-1919.	10.3	49
21	Molecule occupancy by a <i>n</i> -butylamine treatment to facilitate the conversion of Pbl <sub>2</sub> to perovskite in sequential deposition. Physical Chemistry Chemical Physics, 2020, 22, 981-984.	2.8	4
22	Fluorinated hybrid solid-electrolyte-interphase for dendrite-free lithium deposition. Nature Communications, 2020, 11, 93.	12.8	312
23	High-energy plasma activation of renewable carbon for enhanced capacitive performance of supercapacitor electrode. Electrochimica Acta, 2020, 362, 137148.	5.2	31
24	Tailoring the Grain Boundaries of Wideâ€Bandgap Perovskite Solar Cells by Molecular Engineering. Solar Rrl, 2020, 4, 2000384.	5.8	15
25	Structural Regulation for Highly Efficient and Stable Perovskite Solar Cells via Mixed-Vapor Deposition. ACS Applied Energy Materials, 2020, 3, 6544-6551.	5.1	10
26	Rearâ€Illuminated Perovskite Photorechargeable Lithium Battery. Advanced Functional Materials, 2020, 30, 2001865.	14.9	31
27	Synthesis of Au@ZIF-8 nanocomposites for enhanced electrochemical detection of dopamine. Electrochemistry Communications, 2020, 114, 106715.	4.7	97
28	Superstable copper nanowire network electrodes by single-crystal graphene covering and their applications in flexible nanogenerator and light-emitting diode. Nano Energy, 2020, 71, 104638.	16.0	35
29	The electronic properties tuned by the synergy of polaron and d-orbital in a Co–Sn co-intercalated α-MoO <sub>3</sub> system. Journal of Materials Chemistry C, 2020, 8, 6536-6541.	5.5	9
30	Phenylhydrazinium Iodide for Surface Passivation and Defects Suppression in Perovskite Solar Cells. Advanced Functional Materials, 2020, 30, 2000778.	14.9	103
31	Massive Growth of Graphene Quartz Fiber as a Multifunctional Electrode. ACS Nano, 2020, 14, 5938-5945.	14.6	43
32	Flexible 3D Cu/C Scaffolds As Lithium Host for Dendrite-Free Lithium Metal Battery. ECS Meeting Abstracts, 2020, MA2020-02, 3787-3787.	0.0	0
33	Ultrathin Bilayer of Graphite/SiO <sub>2</sub> as Solid Interface for Reviving Li Metal Anode. Advanced Energy Materials, 2019, 9, 1901486.	19.5	128
34	The distinctive phase stability and defect physics in CsPbI <sub>2</sub> Br perovskite. Journal of Materials Chemistry A, 2019, 7, 20201-20207.	10.3	64
35	Graphene photonic crystal fibre with strong and tunable light–matter interaction. Nature Photonics, 2019, 13, 754-759.	31.4	127
36	Ultrafast Catalyst-Free Graphene Growth on Glass Assisted by Local Fluorine Supply. ACS Nano, 2019, 13, 10272-10278.	14.6	32

#	Article	IF	CITATIONS
37	High-performance carbon electrode-based CsPbI2Br inorganic perovskite solar cell based on poly(3-hexylthiophene)-carbon nanotubes composite hole-transporting layer. Journal of Colloid and Interface Science, 2019, 555, 180-186.	9.4	58
38	Capacity Revival of Tungsten trioxide Anode Material in Lithium-Ion Battery. , 2019, , .		0
39	Size and crystallinity control of dispersed VO <sub>2</sub> particles for modulation of metal–insulator transition temperature and hysteresis. CrystEngComm, 2019, 21, 5749-5756.	2.6	16
40	A review on strategies addressing interface incompatibilities in inorganic all-solid-state lithium batteries. Sustainable Energy and Fuels, 2019, 3, 3279-3309.	4.9	83
41	SnO2 Nanoparticles Embedded Biochar as Anode Material in Lithium Ion Batteries. , 2019, , .		1
42	Thermal and illumination effects on a Pbl <sub>2</sub> nanoplate and its transformation to CH <sub>3</sub> NH <sub>3</sub> Pbl <sub>3</sub> perovskite. CrystEngComm, 2019, 21, 736-740.	2.6	4
43	Improving photovoltaic performance of carbon-based CsPbBr3 perovskite solar cells by interfacial engineering using P3HT interlayer. Journal of Power Sources, 2019, 432, 48-54.	7.8	94
44	The novel transistor and photodetector of monolayer MoS2 based on surface-ionic-gate modulation powered by a triboelectric nanogenerator. Nano Energy, 2019, 62, 38-45.	16.0	46
45	Nitrogen-doped graphdiyne nanowall stabilized dendrite-free lithium metal anodes. Journal of Materials Chemistry A, 2019, 7, 27535-27546.	10.3	28
46	Modeling of Charge Transfer in Mesoscopic Perovskite Solar Cells by Considering a Trapassisted Interface. , 2019, , .		1
47	Flower-shaped lithium nitride as a protective layer via facile plasma activation for stable lithium metal anodes. Energy Storage Materials, 2019, 18, 389-396.	18.0	149
48	Research progress of solution processed all-inorganic perovskite solar cell. Wuli Xuebao/Acta Physica Sinica, 2019, 68, 158806.	0.5	4
49	Scalable chemical-vapour-deposition growth of three-dimensional graphene materials towards energy-related applications. Chemical Society Reviews, 2018, 47, 3018-3036.	38.1	140
50	Fabrication of PANI-coated ZnFe2O4 nanofibers with enhanced electrochemical performance for energy storage. Electrochimica Acta, 2018, 273, 282-288.	5.2	36
51	Switching Vertical to Horizontal Graphene Growth Using Faraday Cageâ€Assisted PECVD Approach for Highâ€Performance Transparent Heating Device. Advanced Materials, 2018, 30, 1704839.	21.0	62
52	A strategic review on processing routes towards highly efficient perovskite solar cells. Journal of Materials Chemistry A, 2018, 6, 2406-2431.	10.3	179
53	Low-dimensional perovskite interlayer for highly efficient lead-free formamidinium tin iodide perovskite solar cells. Nano Energy, 2018, 49, 411-418.	16.0	184
54	Mineralâ€Templated 3D Graphene Architectures for Energyâ€Efficient Electrodes. Small, 2018, 14, e1801009.	10.0	21

#	Article	IF	CITATIONS
55	Solution-processed all-oxide bulk heterojunction solar cells based on CuO nanaorod array and TiO2nanocrystals. Nanotechnology, 2018, 29, 215403.	2.6	7
56	Growth of defect-engineered graphene on manganese oxides for Li-ion storage. Energy Storage Materials, 2018, 12, 110-118.	18.0	26
57	Rapid and Low-Temperature Processing of Mesoporous and Nanocrystalline TiO <sub>2</sub> Film Using Microwave Irradiation. ACS Applied Energy Materials, 2018, 1, 6288-6294.	5.1	9
58	Inverted Current–Voltage Hysteresis in Perovskite Solar Cells. ACS Energy Letters, 2018, 3, 2457-2460.	17.4	84
59	Highly Conductive Nitrogen-Doped Graphene Grown on Glass toward Electrochromic Applications. ACS Applied Materials & Interfaces, 2018, 10, 32622-32630.	8.0	37
60	Enhanced photovoltage for inverted planar heterojunction perovskite solar cells. Science, 2018, 360, 1442-1446.	12.6	1,221
61	Self-recovery in Li-metal hybrid lithium-ion batteries <i>via</i> WO <sub>3</sub> reduction. Nanoscale, 2018, 10, 15956-15966.	5.6	87
62	Bias-Dependent Normal and Inverted <i>J</i> – <i>V</i> Hysteresis in Perovskite Solar Cells. ACS Applied Materials & Interfaces, 2018, 10, 25604-25613.	8.0	77
63	Comparison of performance and optoelectronic processes in ZnO and TiO2 nanorod array-based hybrid solar cells. Applied Surface Science, 2018, 456, 124-132.	6.1	18
64	Highly Efficient Perovskite Solar Cell Photocharging of Lithium Ion Battery Using DC–DC Booster. Advanced Energy Materials, 2017, 7, 1602105.	19.5	128
65	Pinhole-Free Hybrid Perovskite Film with Arbitrarily-Shaped Micro-Patterns for Functional Optoelectronic Devices. Nano Letters, 2017, 17, 3563-3569.	9.1	57
66	Fabrication of compact and stable perovskite films with optimized precursor composition in the fast-growing procedure. Science China Materials, 2017, 60, 608-616.	6.3	12
67	Dualâ€Source Precursor Approach for Highly Efficient Inverted Planar Heterojunction Perovskite Solar Cells. Advanced Materials, 2017, 29, 1604758.	21.0	142
68	Oneâ€Step Growth of Graphene/Carbon Nanotube Hybrid Films on Sodaâ€Lime Glass for Transparent Conducting Applications. Advanced Electronic Materials, 2017, 3, 1700212.	5.1	17
69	Activation of Passive Nanofillers in Composite Polymer Electrolyte for Higher Performance Lithium″on Batteries. Advanced Sustainable Systems, 2017, 1, 1700043.	5.3	26
70	Charge Carrier Balance for Highly Efficient Inverted Planar Heterojunction Perovskite Solar Cells Based on Interface Engineering. , 2016, , .		0
71	Mesoporous Pbl <sub>2</sub> Scaffold for Highâ€Performance Planar Heterojunction Perovskite Solar Cells. Advanced Energy Materials, 2016, 6, 1501890.	19.5	124
72	Inverted Perovskite Solar Cells: Progresses and Perspectives. Advanced Energy Materials, 2016, 6, 1600457.	19.5	387

#	Article	IF	CITATIONS
73	Perovskite Solar Cells: High-Performance Inverted Planar Heterojunction Perovskite Solar Cells Based on Lead Acetate Precursor with Efficiency Exceeding 18% (Adv. Funct. Mater. 20/2016). Advanced Functional Materials, 2016, 26, 3551-3551.	14.9	6
74	Scalable Seashell-Based Chemical Vapor Deposition Growth of Three-Dimensional Graphene Foams for Oil–Water Separation. Journal of the American Chemical Society, 2016, 138, 6360-6363.	13.7	212
75	Charge arrier Balance for Highly Efficient Inverted Planar Heterojunction Perovskite Solar Cells. Advanced Materials, 2016, 28, 10718-10724.	21.0	214
76	Growing three-dimensional biomorphic graphene powders using naturally abundant diatomite templates towards high solution processability. Nature Communications, 2016, 7, 13440.	12.8	93
77	Highâ€Performance Inverted Planar Heterojunction Perovskite Solar Cells Based on Lead Acetate Precursor with Efficiency Exceeding 18%. Advanced Functional Materials, 2016, 26, 3508-3514.	14.9	176
78	Bioinspired synthesis of CVD graphene flakes and graphene-supported molybdenum sulfide catalysts for hydrogen evolution reaction. Nano Research, 2016, 9, 249-259.	10.4	24
79	Catalyst-Free Growth of Three-Dimensional Graphene Flakes and Graphene/g-C <sub>3</sub> N <sub>4</sub> Composite for Hydrocarbon Oxidation. ACS Nano, 2016, 10, 3665-3673.	14.6	122
80	Electrospun synthesis and electrochemical property of zinc ferrite nanofibers. Ionics, 2016, 22, 967-974.	2.4	13
81	Direct Synthesis of Few‣ayer Graphene on NaCl Crystals. Small, 2015, 11, 6302-6308.	10.0	57
82	Sonochemical synthesis and high lithium storage properties of Sn/CMK-3 nanocomposites. Electrochimica Acta, 2015, 165, 149-154.	5.2	9
83	Fabrication of electrospun ZnMn 2 O 4 nanofibers as anode material for lithium-ion batteries. Electrochimica Acta, 2015, 177, 283-289.	5.2	44
84	Electrospun synthesis and lithium storage properties of magnesium ferrite nanofibers. Electrochimica Acta, 2015, 160, 43-49.	5.2	43
85	Uniform single-layer graphene growth on recyclable tungsten foils. Nano Research, 2015, 8, 592-599.	10.4	18
86	Facile synthesis of one-dimensional zinc vanadate nanofibers for high lithium storage anode material. Journal of Alloys and Compounds, 2015, 649, 1019-1024.	5.5	42
87	A highly efficient, orange light-emitting (K <sub>0.5</sub> Na <sub>0.5</sub> )NbO <sub>3</sub> :Sm <sup>3+</sup> /Zr <sup>4+</sup> lead-free piezoelectric material with superior water resistance behavior. Journal of Materials Chemistry C, 2015. 3. 5275-5284.	5.5	54
88	Amino-functionalized magnetic magnesium silicate double-shelled hollow microspheres for enhanced removal of lead ions. RSC Advances, 2015, 5, 22973-22979.	3.6	21
89	Low temperature pseudomorphic synthesis of nanocrystalline carbide aerogels for electrocatalysis. Journal of Materials Chemistry A, 2015, 3, 11745-11749.	10.3	12
90	Fast-growing procedure for perovskite films in planar heterojunction perovskite solar cells. Chinese Chemical Letters, 2015, 26, 1518-1521.	9.0	16

#	Article	IF	CITATIONS
91	A universal etching-free transfer of MoS2 films for applications in photodetectors. Nano Research, 2015, 8, 3662-3672.	10.4	94
92	Direct low-temperature synthesis of graphene on various glasses by plasma-enhanced chemical vapor deposition for versatile, cost-effective electrodes. Nano Research, 2015, 8, 3496-3504.	10.4	112
93	Laccase Biosensor Based on Electrospun Copper/Carbon Composite Nanofibers for Catechol Detection. Sensors, 2014, 14, 3543-3556.	3.8	61
94	Template confined synthetic strategy for three-dimensional free-standing hierarchical porous nanocrystalline tantalum. Materials Letters, 2014, 116, 31-34.	2.6	6
95	High lithium electroactivity of electrospun CuFe2O4 nanofibers as anode material for lithium-ion batteries. Electrochimica Acta, 2014, 144, 85-91.	5.2	74
96	Synthesis and characterization of carbide nanosheets by a template-confined reaction. Journal of Nanoparticle Research, 2012, 14, 1.	1.9	9
97	Reduced graphene oxide paper by supercritical ethanol treatment and its electrochemical properties. Applied Surface Science, 2012, 258, 5299-5303.	6.1	45
98	Potential SiO2/CRF bilayer perturbation aerogel target for ICF hydrodynamic instability experiment. Fusion Engineering and Design, 2012, 87, 92-97.	1.9	7
99	Freestanding monolithic silicon aerogels. Journal of Materials Chemistry, 2012, 22, 16196.	6.7	58
100	One-pot synthesis, characterization and properties of acid-catalyzed resorcinol/formaldehyde cross-linked silica aerogels and their conversion to hierarchical porous carbon monoliths. Journal of Sol-Gel Science and Technology, 2012, 62, 294-303.	2.4	27
101	Synthesis of resorcinol–formaldehyde/silica composite aerogels and their low-temperature conversion to mesoporous silicon carbide. Microporous and Mesoporous Materials, 2012, 149, 16-24.	4.4	65
102	Design and fabrication of a CH/CRF dual-layer perturbation target for ICF hydrodynamic experiments. Nuclear Fusion, 2011, 51, 083044.	3.5	5
103	Dynamics analysis of erythrosine B sensitized photopolymer holographic gratings. , 2008, , .		0
104	Comparison of high-density holographic characteristics of photopolymers sensitized by two kinds of thiazine dyes. , 2008, , .		0